RSC Advances

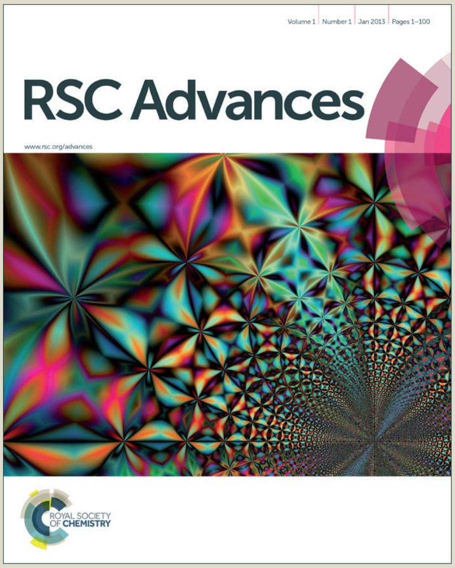

ROYAL SOCIETY OF CHEMISTRY

www.rsc.org/advances

Synthesis and Characterization of Graphene and Functionalized Graphene via Chemical and Thermal Treatment Methods

Behzad Dehghanzad[a,b], Mir Karim Razavi Aghjeh*[a,b], Omid Rafeie[a,b], Akram Tavakoli[c] and Amin Jameie Oskooie[a,b]

[a]Institute of Polymeric Materials, Sahand University of Technology, Sahand New Town, Tabriz, Iran,
P.C: 51335-1996

[b]Faculty of Polymer Engineering, Sahand University of Technology Sahand New Town, Tabriz, Iran,
P.C: 51335-1996

[c]Faculty of Chemical Engineering, Sahand University of Technology Sahand New Town, Tabriz, Iran,
P.C: 51335-1996

*Correspondence to: Dr. M.K. Razavi Aghjeh
Email: karimrazavi@sut.ac.ir

Abstract

Graphene oxide was successfully synthesized via oxidation of graphite, functionalized with dodecyl amine and then chemically reduced using hydrazine hydrate. The graphene oxide was also thermally reduced and exfoliated to obtain graphene. Different characterization methods including elemental, FTIR, XPS, Raman, TGA and XRD analyses were employed to deeply analyze the structure of the resulted materials. The results of different analysis mostly supported each other and demonstrated that different oxygen containing functional groups, those which were capable to grafting of dodecyl amine chains, have been created on the surface of graphite during the oxidation process at the expense of the increased defects. Chemically reduction using the hydrazine hydrate led to low extent of oxygenic groups and defects as well as increased graphitization. It was also shown that dodecyl amine plays the role of a reduction agent during functionalization process. Thermally treatment of graphene oxide resulted in graphene structure. Structural alterations of different synthesized and functionalized materials were well reflected in their amphiphilic characteristic and morphological features, evaluated using the contact angle experiments and SEM analysis, respectively.

Keywords: Graphene, Graphene Oxide, Functionalization, Dodecyl amine, Characterization

1. Introduction

Graphene is the latest member of the nano-carbon family, with 2D single layer of carbon atoms having the hexagonal packed structure.[1] Graphene-based platelets show promise for a variety of potential applications and for this reason the researchers in many scientific disciplines are interested in these materials.[2] There is of great interest to graphene as reinforcement to structural composites, due to its excellent mechanical properties, 1 TPa elastic modulus and 130 GPa tensile strength, those which led to its nickname of "super carbon".[3, 4]

Graphene-based polymer composites are usually fabricated by solution mixing of nano-fillers and polymer matrixes.[5-8] However, the homogeneous dispersion of the graphene platelets through the polymeric matrixes and providing the efficient interfacial interaction between them are still the main challenges for this method due to the strong tendency of the graphene sheets to restacking and/or aggregation.[9] Functionalization of graphene nano-platelets, physically or chemically to improve the interfacial interactions between graphene sheets and polymer matrixes is an efficient strategy for fabricating graphene based polymer composites.[10, 11]

Graphene can be prepared or synthesized from the graphite source by using different mechanical or chemical treatment methods.[12] The key point in the preparation of graphene from graphite sources is delamination of graphite sheets and prevention of their restacking during the processes. Restacking of the graphene sheets can be prevented or reduced via the chemical bonding of some polymeric or oligomeric chains on to its surface.[13, 14] As there are any reactive groups on the surface of graphite, the grafting of functional groups cannot be taken place unless the surface is oxidized to create different reactive oxygen containing groups before than grafting process. Chemical oxidation and exfoliation of graphite is one of the most important routs to prepare graphene oxide (GO).[15, 16] The GO has abundant functional groups on its surface and edge including hydroxyls, epoxides, diols, ketones and carboxyls, [8, 17, 18] which provide more reactive sites for covalent functionalization.[19, 20] Moreover, the chemical functional modification significantly alters the Van der Waals interactions among the nano-filler aggregates, making them easy to be dispersed in the polymer matrix.[21, 22] For instance, Roghani-Mamaqani et al.[18, 23] established a well-defined process to graft polystyrene chains with various graft densities at the edge of GO nano-sheets. Samadaei et al.[24] functionalized GO by ethylenediamine and poly (amidoamine). Kuila et al.[25] prepared the functionalized graphene (ODA-GO) and then studied the mechanical behaviors of ODA-G/EVA composites. Peng et al.[26] prepared GO and dodecyl amine functionalized graphene/polyethylene nano-composites.

The main objective of our research was to study on the microstructure and rheological properties of graphene based polyethylene blend nano-composites. At the first step it was tried to functionalize the graphene oxide, prepared via oxidation of graphite, with an alkyl chain containing material (dodecyl amine) to increase its interaction with polyethylene. [27] The resulted modified materials were used in the preparation of polyethylene blend nano-composites, at the second step. In this part, we presented the procedures of preparation of graphene oxide (GO), functionalized graphene oxide with dodecyl amine (FGO) and reduced functionalized graphene oxide (RFGO). Different characterization methods were employed to deeply characterize the structural changes and alteration of the morphology of the source materials during different modification processes. Thermal treatment method [28, 29] was also used to rapidly reduce the GO to obtain thermally reduced graphene (TRG) and the characteristics were compared with those of RFGO sample. Rheology and morphology of graphene based polyethylene blend nano-composites will be the subject of the next study.

2. Experimental

2.1. Materials

Natural graphite flakes and hydrazine hydrate were purchased from Merck. Dodecyl amine (purity of 99.0%), pyridine and triethylamine were purchased from Sigma Aldrich Co. Sulfuric acid (H_2SO_4, purity of 98%), phosphoric acid (H_3PO_4), hydrochloric acid (HCl, purity of 37%), hydrogen peroxide (H_2O_2, purity of 30%), potassium permanganate ($KMnO_4$) and ethanol (purity of 99.8%) were provided from Dr. Mojalali Co. N,N-dimethyl formamide (DMF, purity of 99.5%) was supplied by Daejung Co.

2. 2. Synthesis procedures

Synthesis of graphene oxide (GO)

Graphene oxide sheets were synthesized by exfoliating the natural graphite with a strong oxidative acid mixture using improved hummers' method [30, 31] as follows:

Natural graphite flake (7.5 g) was oxidized in a solution of H_2SO_4 and H_3PO_4 (9:1 ratio, 360 ml) in an ice bath for about 5 h and then 45 g of $KMnO_4$ was slowly added to the mixture and stirred for about 15 h, while the temperature was kept below 35 °C. Finally, H_2O_2 (90 ml) and HCL (10%, 100 ml) were slowly added to the mixture, while stirred for 0.5

h in an ice bath, because of exothermic nature of reaction in this stage.[32] The produced graphite oxide was then dispersed in DI water and sonicated. Finally, the mixture was centrifuged for about 1 h and the resulted graphene oxide was dried overnight in a vacuum oven at 80 °C.

Preparation of reduced graphene oxide (RGO)

1 g of graphene oxide (GO) powder was added to a flask containing of 200 ml purified water and then 6 ml of hydrazine hydrate was immediately added and the mixture was stirred for 5 h under reflux, while the flask was immersed in an oil bath at 80 °C. The resulting black powder was filtered and dried following the same method as for GO. The final dried product was marked RGO.

Synthesis of functionalized graphene oxide (FGO)

2.5 g of graphene oxide (GO) and 2.6 g of dodecyl amine were dispersed in 200 ml of DMF and the mixture was sonicated for 2 h. Then 8 ml of triethylamine and 1 ml of pyridine were added to the mixture and stirred for 72 h at 95 °C in the nitrogen atmosphere, under reflux. The product was then dispersed in the solution of DMF and ethanol to remove unreacted dodecyl amine. Finally the mixture was centrifuged and the sediment was dried overnight in a vacuum oven at 55 °C. The final dried product was marked FGO.

Preparation of reduced functionalized graphene oxide (RFGO)

1 g of the functionalized graphene oxide (FGO) was dispersed in 200 ml solution of ethanol and water (1:1 ratio) and then the mixture was sonicated for 1 h. Then 6 ml of hydrazine hydrate was added and the reaction was performed at 95 °C for about 5 h, under reflux. The end product (RFGO) was washed by a solution of water and ethanol to remove the excess hydrazine hydrate and then dried in a vacuum oven at 55 °C, overnight.[33, 34]

Preparation of thermally reduced graphene oxide (TRG)

The exfoliated graphene sheets were also prepared directly via rapid thermal treatment of the GO sample. About 1.5 g of GO sample was placed in a furnace for about 1 min at temperature of 1050 °C and nitrogen atmosphere to split the GO sample into individual sheets through evolution of CO_2[33, 35] and then was quickly cooled down to store the amorphous nature of the exfoliated carbon sheets. The final product was marked TRG.

2.3. Characterizations

C, H and O content analysis of Go sample was carried out using a Multi EA 3100 analyzer (Analytica jena, Germany CHNSO analyzer). Prior to the elemental analysis the sample was heated at 80 °C under vacuum to remove adsorbed solvents.

Fourier transforms infrared spectroscopy (FTIR) measurements were performed on a Tensor 27, Germany, FTIR spectrometer over the wave number range of 400–4000 cm^{-1} by 24 scans at a resolution of 4 cm^{-1} with 30 sec interval to minimize the effects of dynamic scanning. In FTIR experiments the KBR substrate was used and the background data subtraction was applied with FTIR device.

XPS analysis was performed by XSAM800 (Kratos company, Britain) using Al (1486.6 eV) and Mg (1253.6 eV) radiation. CasaXPS2316PR1 software was used to perform curve fitting, deconvolution and calculation of the atomic ratios.

To evaluate the changes in the hydrophilicity of the GO sample after chemical modification and reduction by different methods, the contact angle analysis was performed. The samples were dispersed in DI water (0.1 g/lit) and sonicated for 1 h. Then a required amount of the resulting solution was placed in the HPLC filters made of Teflon by a mesh size of 0.2 µm and dried for 24 h at room temperature. 0.5 µL of DI water droplet was released onto product surface from a syringe needle. The image of the liquid droplet was obtained in real time by using a CCD camera (1.3 MP). The contact angle data of three measurements per sample were evaluated by Image J software.

Raman spectroscopy was performed at room temperature using a Raman microscope SENTRA (Bruker, Germany). It had 2µm confocal depth resolution to analyze the microstructure and morphology of the samples at the point (spectral resolution < 3 cm^{-1}, CCD detector, spectral range 90-3500 cm^{-1} and 785 nm excitation source).

The crystalline structures of the samples were investigated with XRD technique using a Philips diffractometer with Cu anode irradiation (λ= 1.541 °A). X-ray diffraction measurements were performed directly on the powder samples at a scanning rate of 0.03°/min and step time of 0.3 sec in 2θ range of 3 to 30°.

Thermogravimetric analysis was carried out with STA PT1600 (Linseis, Germany) thermogravimetric analyzer. The heating rate was 10°C/min under nitrogen atmosphere from room temperature up to 600°C.

Scanning electron microscopy (SEM) images were obtained using a JEOL JSM 840A microscope by mounting the sample on conducting carbon tape and sputter coating with gold.

3. Result and Discussion

The results of elemental analysis showed that the GO sample contains 48.3, 2.21 and 49.6% of C, H and O, respectively. The value of C/O ratio (0.98) was used in the computing of the amount of dodecyl amine for functionalization of GO.

Fig. 1 shows the FTIR spectra of different synthesized samples along with pure graphite. The existence of the characteristic peaks at 1260 and 1730 cm^{-1} wave numbers, which are related to ester bond formed in the results of reaction between the carboxylic acid of GO sheets and the amine groups of dodecyl amine, provides direct evidence for covalent bonding between GO's carboxylic acid groups and dodecyl amine chains. Moreover, the transmittance peaks appeared at the wave numbers of 1300, 1550, 1373, which are corresponded to the bending of C-N, C=N, CH_3 groups of dodecyl amine, respectively, illustrate covalent bonding between GO sheets and dodecyl amine chains.

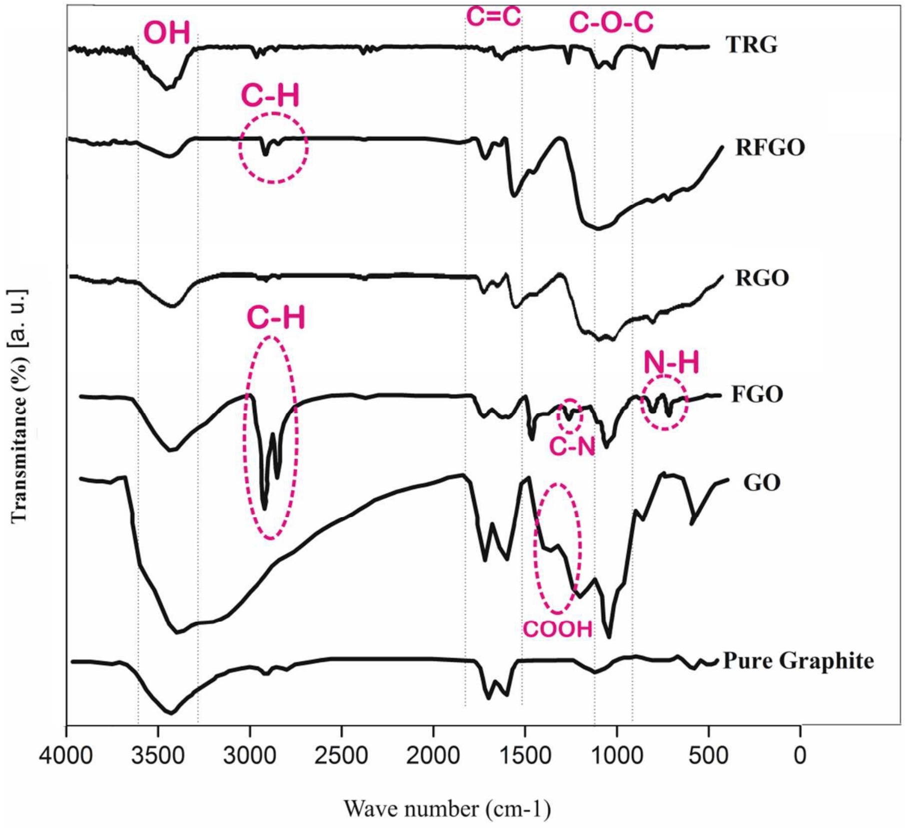

Fig. 1: FTIR spectra of different synthesized samples along with pure graphite.

At the other extreme, as it is clearly obvious, the intensity of all oxygenic groups related peaks significantly reduced after functionalization with dodecyl amine. It was attributed to the reduction effect of NH_2 functional groups of dodecyl amine. The same results have been reported by Samadae et. al,[24] when graphene oxide has been treated with ethylenediamine modifier. The comparison between the spectrums of the RFGO and FGO samples shows that the intensity of characteristic peaks of RFGO has been decreased, which was attributed to the reduction and removal of oxygen containing groups in RFGO sample. The structures of the FGO and RFGO samples are schematically depicted in **Fig. 2**. The FTIR spectrum of TRG sample shows that the TRG structure is closer to graphite.

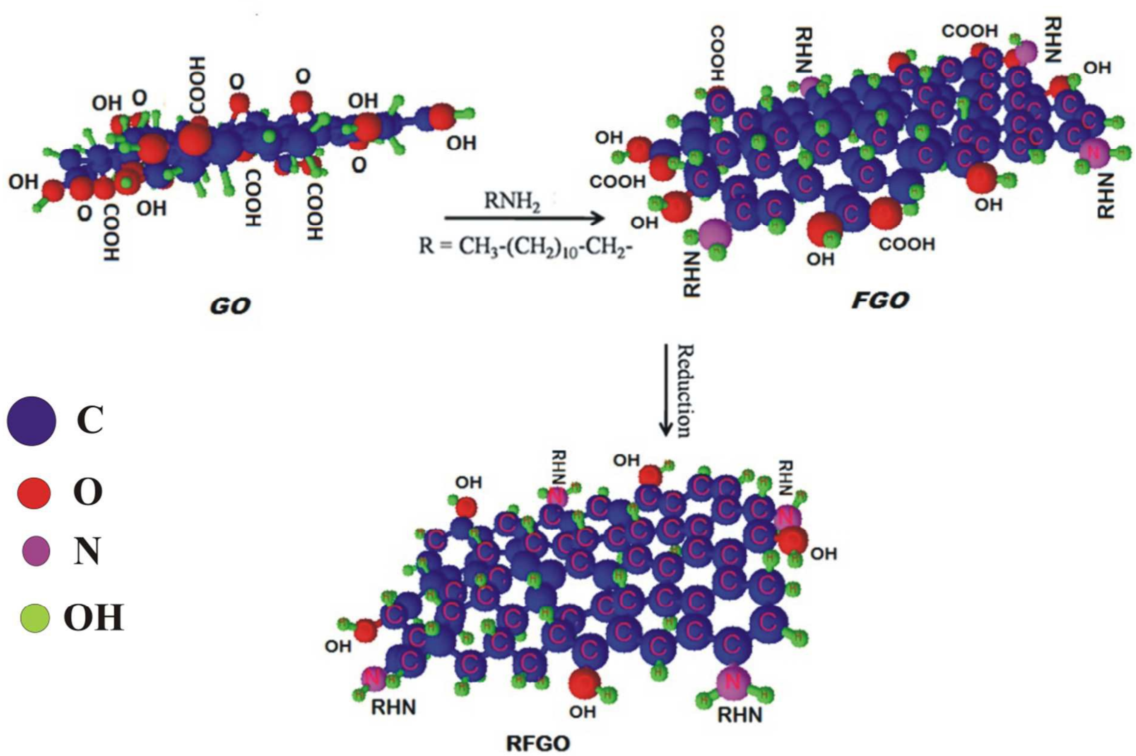

Fig. 2: Schematic of the structure of the FGO and RFGO samples.

The XPS spectra were analyzed to further identify the chemical composition of the surfaces and possible changes in the surface characteristics of the GO, FGO and RFGO samples. The wide scan spectrums for GO, FGO and RFGO samples are shown in **Fig. 3.** The deconvoluted spectrums are presented in supplementary materials for different samples (**Figs. S1 - S3**). The C (1s), O (1s) and N (1s) peak positions and their relative atomic percentages for all the samples, obtained from deconvoluted spectrums, are listed in **Table I.**

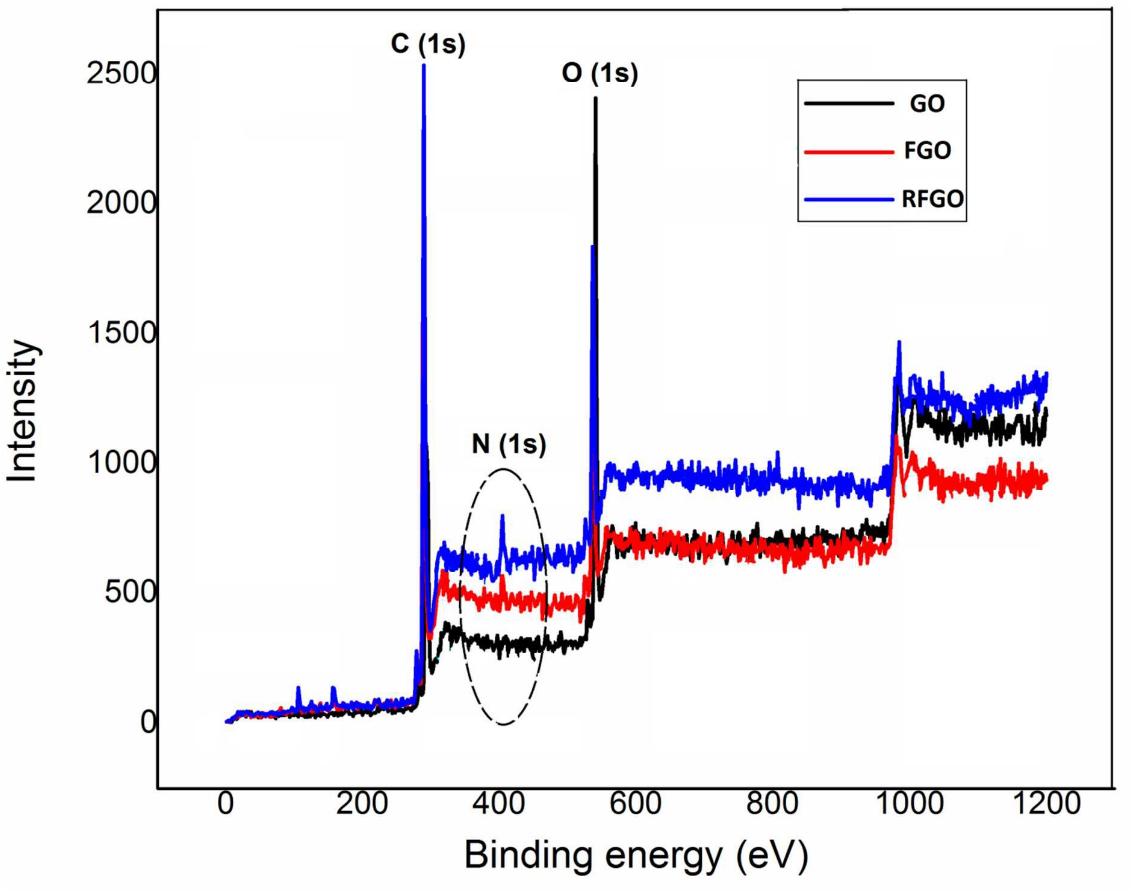

Fig. 3: XPS wide scan spectrums of GO, FGO and RFGO samples.

The GO sample shows considerable degree of oxidation with 5 types of carbon atoms in different functional groups: C=C (284.54 eV), C-OH (285.54 eV), C-O-C (286.3 eV), C=O (287.9 eV) and HO-C=O (289 eV) concluded from C (1s) spectrum (**Fig. S1)**. Also, O (1s) spectrum of GO sample showed 5 groups C=O (529.2 eV), OH-C=O* (530.1 eV), C-OH (531.9 eV), C-O-C (532eV) and O=C-O*H (533 eV). C (1s) band spectra in the binding energy region of 282–290 eV was used to evaluate the proportion of various carbon-containing functional groups in different samples. Also, undoubtedly, the existence of C-C peak in FGO sample (**Fig. S2)** reflects the success of grafting process on GO sample. Appearance of C–C peak at the binding energy of 284.8 eV for FGO sample shows that alkyl groups have successfully been attached to the carboxyl and/or epoxy groups, which was attributed to the ester and ether linkages.[35-37]

The O (1s) spectrum for FGO sample shows that two new peaks at 532 and 534 eV have been appeared compared to GO sample. These peaks are corresponded to oxygen's of ether and ester groups, respectively, which confirm the grafting of dodecyl amine on the GO sample during functionalization process.[26, 36]

Table I. XPS spectrum data of GO, FGO and RFGO samples C (1s), O (1s) and N (1s) (wt. %).

Sample/ (C 1s)	C/O	C=C	C-C	C-OH	C-O-C	C=O	OH-C=O
GO	1.07	51.89	-	30.11	7.8	1.11	9.09
FGO	0.92	10.83	31.56	20.35	8.28	10.90	18.07
RFGO	2.2	27.58	41.2	11.83	12.35	1.98	5.06
Sample/ (O 1s)	**C=O**	**OH-C=O***	**C-O-R**	**C-OH**	**C-O**	**O=C-O*R**	**O=C-O*H**
GO	2.34	2.1	-	51.6	12.7	-	31.26
FGO	3.3	20.1	34.05	4.82	17.3	6.92	13.51
RFGO	8.4	9.74	24.58	2.41	19.9	26.11	8.86
Sample/ (N 1s)		**C-N/ C=N**			**N-H**		
GO		-			-		
FGO		73.30			26.70		
RFGO		56.37			43.63		

Appearance of N (1s) peak in FGO spectra such as C-N (399.5 eV), C=N (399.5 eV), N-H (402 eV) groups is another evidence for grafting of dodecyl amine groups on GO sheets. As it can be seen in **Table I** the atomic percentage of C-OH significantly reduced from 51.6 (GO) to 4.82(FGO) in the results of functionalization. This shows that the hydroxyl groups of GO have been converted to H_2O during the grafting reaction. This confirms one more time that the amine group of dodecyl amine chains acts as a reduction agent. Higher peak area and peak intensity of C (1s) for RFGO sample (**Fig. S3**) compared to the FGO sample (**Fig. S2**) is originated from its high carbon content. It can be attributed to successfully reduction phenomenon taken place by hydrazine hydrates as a redaction agent. As a result, sp^3 hybridization returned to sp^2 form.

The contact angle analysis was used to assessment of hydrophilicity/hydrophobicity of the various samples. **Fig. S4** in supplementary materials shows images of contact angle test for all the samples. Pure graphite exhibits as hydrophobic material by contact angle of 84°, while GO is inherent hydrophilic material with contact angle of 0°. Dodecyl amine with contact angle of 140° is considered as a hydrophobic material because of the alkyl chains. Surface functionalization of GO by dodecyl amine chains increased the contact angle from 0 to 54°, indicating that the presence of hydrophobic groups on FGO surfaces changed its hydrophilic nature, so that the FGO sample was considered as a relative hydrophilic material. Hu et al.[38] reported that the materials with content angles less than 90° exhibit hydrophilic behavior.[36] When FGO sample was reduced by hydrazine hydrate to synthesis the RFGO sample, its surface structure more and less returned to graphite conformations, by means that the contact angle increased from 54° to 61°. Similar results have been reported in other research works.[39] The TRG sample exhibits amphiphilic behavior similar to graphite showing the successful removing of oxygen containing groups in the thermal treatment stage. The contact angel data are in a good agreement with the results obtained from XPS and FTIR analysis.

Fig. 4 represents the thermal stability of different samples, investigated by TGA analysis. The TGA curve of GO sample showed two major weight losses. The first weight loss step, started at about 80 °C, was related to vaporization of the absorbed water on GO sheets, while the second weight loss step, started at about 200 °C, was attributed to the decomposition of oxygen containing functional groups (i.e. C=O, C-O-C and -OH). While the amounts of oxygenic groups was 49.6 wt%., according to elemental analysis, the quantity of decomposed oxygen groups was about 63 %wt., according to TGA analysis. The principal reason of the excess weight loss was related to elimination of carbon atoms of graphene sheets together with the oxygen during the combustion process.

FGO sample showed three weight loss steps at about 100 °C, 200 °C, and 350 °C. Two decomposition steps at 100 and 200°C were attributed to adsorbed water and distraction of oxygen groups, respectively, similar to GO sample. A comparatively small amount (2 wt. %) of weight loss by FGO in this temperature region indicates that FGO does not contain much water as previously reported. The additional weight loss at highest temperature (i.e. 350 °C) was attributed to the decomposition of alkyl groups of dodecyl amine. Assuming the release of only oxygen without carbon elimination, the maximum degree of grafting calculated from TGA curves by analyzing the weight loss between 300-600 °C, is obtained about 30 wt%. This is another evidence for prosperous grafting of alkyl amine groups on GO sheets during the functionalization step. Also, as it can be seen, GO sample had clearly higher weight loss (i.e. about 80 wt. %) than FGO sample (i.e. about 10 wt. %) at the range of 200°C, which was attributed to the reduction effect of NH_2 groups of dodecyl amine.

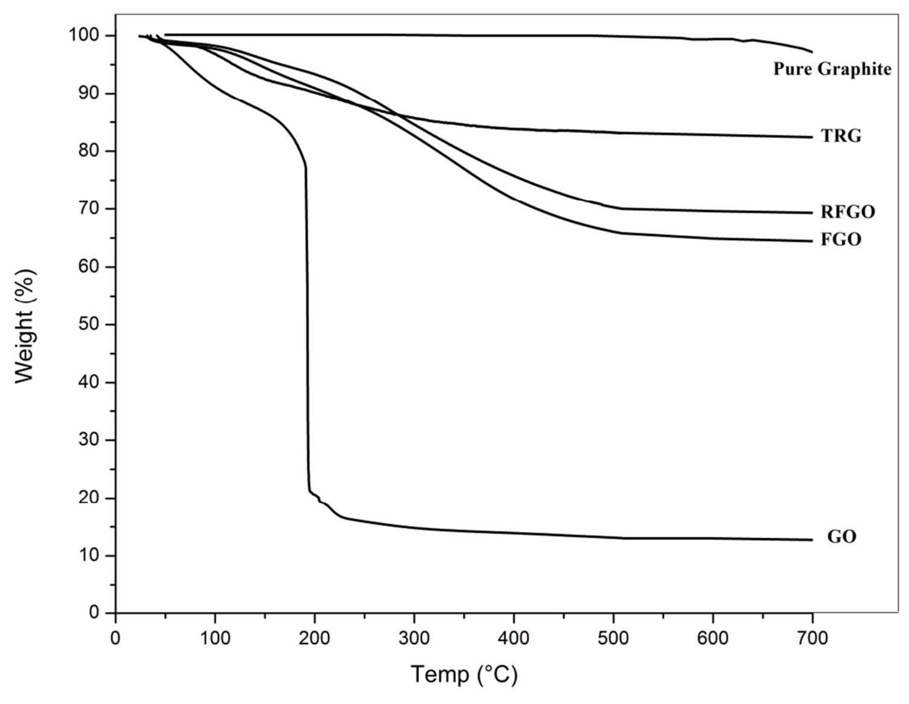

Fig. 4: TGA curves of pure graphite, GO, FGO, RFGO and TRG samples.

Based on TGA data, the RFGO sample exhibits relatively higher thermal stability than FGO sample, which can be attributed to the reduction effect. TRG sample shows much higher thermal stability than that of RFGO sample, but lower than pure graphite. The former is because in TRG sample there are any alkyl groups and the latter shows that TRG sample still contains oxygen groups. Assuming the same oxygen contents of TRG and RFGO samples and comparing their ash contents indicates that the amount of grafted dodecyl amine in RFGO sample is about 15 wt.%. This is much lower than that estimated from comparing the TGA curves of pure graphite and FGO samples, showing that carbon also removes together with oxygen during degradation process. Therefore the real grafting degree of dodecyl amine is about 15 wt%.

Structural changes during the oxidation and exfoliation process can also be followed by Raman spectroscopy.[40] **Fig. 5** shows the Raman spectra of pure graphite, GO, FGO, RFGO and TRG samples and the collected data are presented in **Table II**. As it can be seen, the Raman spectrum of the pure graphite displayed a relatively weak band at 1284 cm^{-1} (D band) and a prominent peak as the feature at 1597 cm^{-1} (G band), which are ascribed to the breathing mode of the symmetry K-point associated with defects in the graphene or graphene edges and the radial C-C stretching mode associated with sp^2 bonded carbon, respectively.[24, 39, 40] The intensity ratio of D band to G band (I_D/I_G), as a measure of the quality of graphitization or defective disorders on the crystalline graphite, was used to determine how the modification processes disrupt the structure of graphite.[24] The I_D/I_G value is obtained almost zero for pure graphite, which shows very low defect region on graphite sheets.

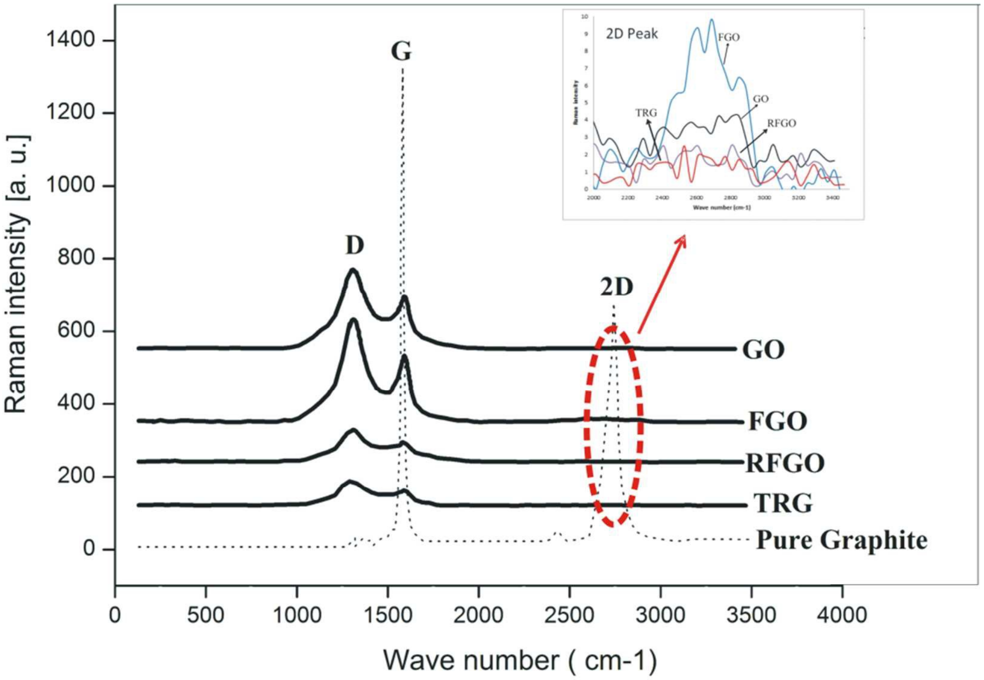

Fig. 5: Raman spectra of pure graphite, GO, FGO, RFGO and TRG samples

Table II. Raman spectroscopy data for different samples

Sample	I_D/I_G	D (cm^{-1})	G (cm^{-1})	L (A°) =44/ (I_D/I_G)
Graphite	-	–	1580	-
GO	1.54	1284	1597	28.57
FGO	1.57	1289	1586	28.02
RFGO	1.6	1330	1582	27.5
TRG	1.75	1290	1580	25.14

The GO sample indicated higher I_D/I_G ratio (I_D/I_G= 1.54), which was attributed to the removal of symmetry between the plates that was affected by increase of defects regions in the result of oxidation. On the other hand, decreasing on the 2D peak (2D=2390 cm^{-1}) intensity, is an indicative of decreasing of the number of graphene layers in GO sample compared to pure graphite sample. The average distance between two neighbor defects (L) was quantified using the following equation, presented by Tuinstra et al.[24, 41] and listed in **Table II**:

$$L\ (A°) = 44/\ (I_D/I_G)$$

Accordingly, increment in I_D/I_G ratio is an indicative of increased the number of defects and decrease the distance between two neighbor defects. Based on this relation, the results showed that oxidation of pure graphite increased the number of structural defects.[42] It can be seen that the G peak of FGO has moved to 1586 cm^{-1}, which was an indicative of the presence of grafted groups and partially reduction of plates. Negligibly increase in I_D/I_G ratio of FGO compared to GO was related to the slightly increased the number of defect regions. Reduction of FGO to obtain RFGO increased slightly I_D/I_G ratio. Moreover the intensity of G and D peaks of RFGO sample are much lower than those of FGO sample. Sasaki et al.[13] reported that breaking of graphene plates could decrease the intensities of G and D peaks. Therefore this decrement can be attributed to the effect of reduction process as well as sever sonication, applied after reduction process. Some of the functional groups (i.e. epoxy, carboxyl, etc.) and surface modifiers (i.e. dodecyl amine) were probably destroyed during reduction process, therefore structural defects decreased and size of plates became more less. On the other hand, the G peak of RFGO shifted to 1582 cm^{-1}, which was attributed to reforming of sp^3 to sp^2 forms. Raman spectrum of TRG sample is almost similar to RFGO sample. However, higher intensity of I_D/I_G ratio in TRG sample, completely disappearance of 2D peak in this sample and the same G peak position of TRG as pure graphite, strongly suggest that TRG sample contain exfoliated graphene nano-sheets.

The exfoliation degree of GO, FGO, and RFGO samples was studied by X-ray diffraction (**Fig. 6)**. The XRD pattern of pure dodecyl amine is also presented in this figure. X-ray diffraction pattern of GO powder shows a larger interlayer spacing than that of graphite (GO, major peak at 2θ = 10.4° corresponding to an interlayer spacing of 8.32 A° compared with graphite's major peak from (002) at 2θ = 26° corresponding to 3.36 A°), due to the oxygen functional groups of GO as well as water molecules held in the interlayer galleries of hydrophilic GO. There are two characteristic peaks in XRD pattern of FGO sample (2θ = 4.5°

and 2θ = 22°). The first peak which appeared slightly higher than peak position of GO sample is because of reduction effect of amine groups. The second peak can also be related to reduction effect and probably to crystallization of grafted dodecyl amine on FGO sheets. The letter was concluded from comparing the XRD patterns of FGO and dodecyl amine. These results confirm the results obtained from FTIR analysis. As it can be seen, the (002) peak at 2ϴ=10.4° has been appeared for the RFGO sample, that ascribed by decrease in plate distance to 7.56 A° and the peak at 2θ =22° for FGO sample has shifted to 2ϴ=24°, for RFGO sample, both as results of reduction process. These results, in conjunction with the results of Raman spectroscopy analysis, confirmed hybridization of sp^3 to sp^2 during the reduction of FGO sample. The XRD pattern of TRG sample is an indicative of completely exfoliated graphene nano-sheets.

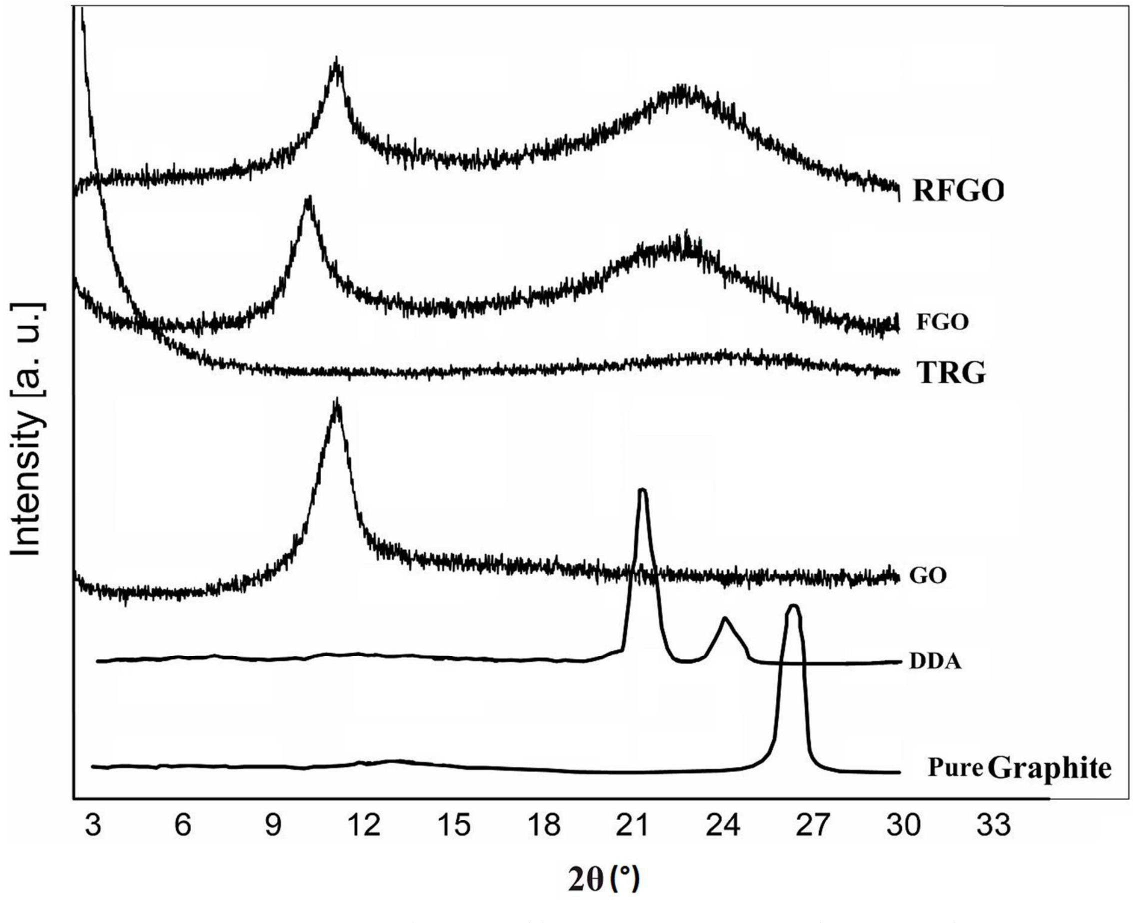

Fig. 6: XRD patterns of pure graphite, GO, FGO, RFGO and TRG samples.

The detailed morphology of all the samples was characterized by direct observation via SEM micrographs, which were shown in **Fig. 7**. For the aim of better visualization high magnificent images were inserted in each image. As can clearly be seen, the graphite used in this study are consisted large agglomerates with thick size, in which the parallel graphite sheets are physically bonded to each other by π- π interactions and are stacked regularly **(Fig. 7a)**. The SEM image of GO (**Fig. 7b**) reveals that oxidation process has effectively broken down the graphite agglomerates to wrinkled aggregates with small size. Also, as it can be seen from high magnifications of this image (see inside image of **Fig. 7b**), the GO sheets shows increased distance between graphite sheets due to the oxidation process which generates oxygen containing functional groups on the surfaces of graphite sheets. A thin layer of dodecyl amine can be seen surrounding the GO sheets (marked by red circles), after its functionalization with dodecyl amine (**Fig. 7c)**.

Also the SEM images of FGO sample (**Fig. 7c**) clearly display that the FGO sample has a rougher wrinkled surface topology. The thickness of FGO aggregates is higher than those of GO sheets, originated from reduction effect of dodecyl amine groups, which caused to a relatively stacked structure. These results indicate that the surface functionalization has successfully changed the surface morphology of the GO sheets. This result proved the results of XRD pattern of FGO samples, where a new peak was appeared at higher 2ϴ. **Fig. 7d** presents a typical SEM image of RFGO aggregates, where a lot of sheets were observed to be roughly connected to each other. The average thickness of RFGO aggregates is much higher than those of the exfoliated GO sheets and FGO samples. The stacking structure of RFGO could be also observed from this image. Since hydrazine primarily reduces both epoxy and hydroxyl groups in graphene oxide, graphitic stacked structure has been returned. This result confirms the XRD pattern of RFGO sample, where the 002 peak of graphitic structure of RFGO sample shifted to higher 2ϴ. After rapid thermal treatment of GO sheets (i.e. TRG sample, see **Fig. 7e**), a significant exfoliation of stacked graphite sheets into thin graphene sheets can be observed.

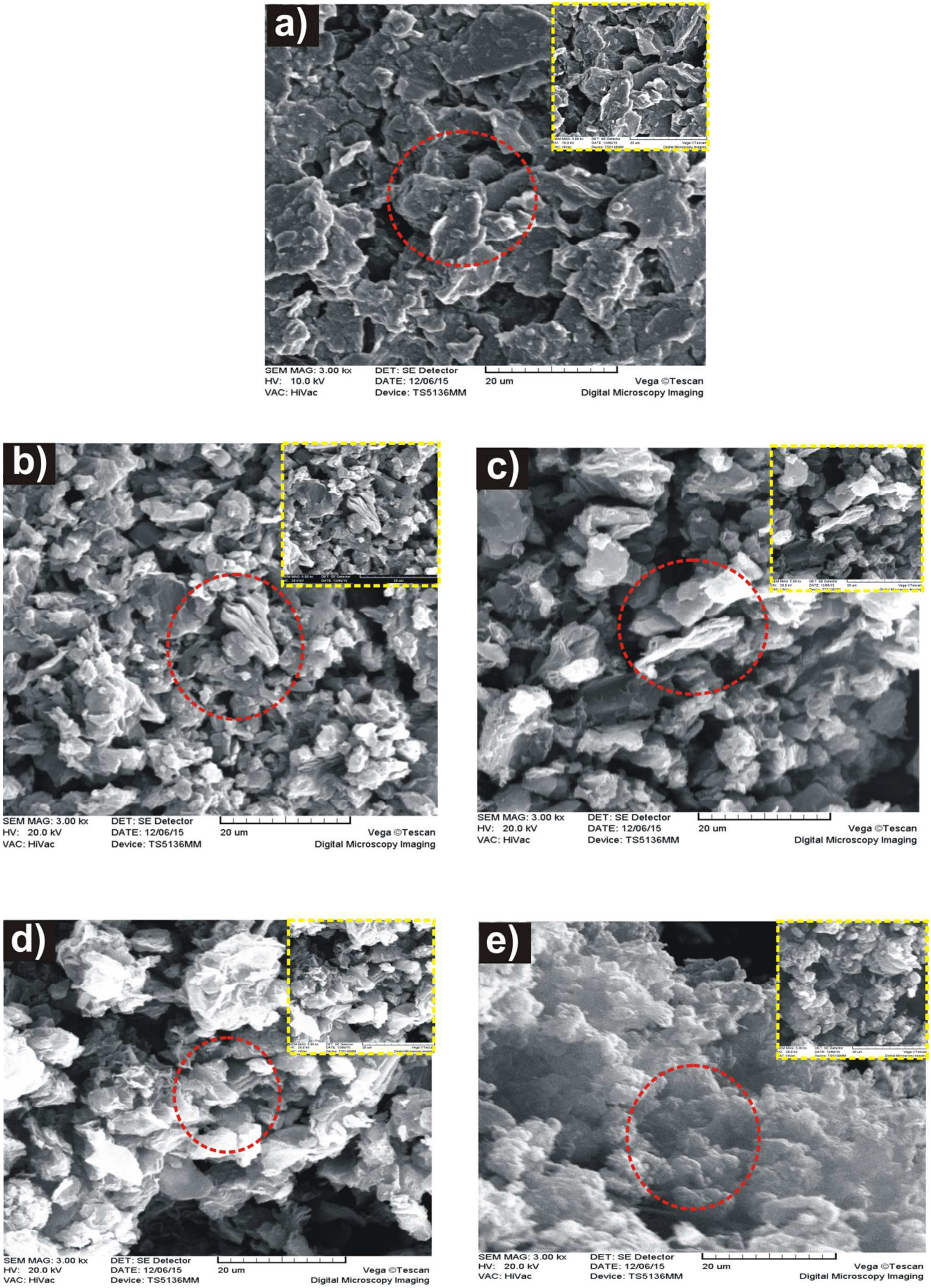

Fig. 7: SEM images of **a**) pure graphite, **b**) GO, **c**) FGO, **d**) RFGO and **e**) TRG samples.

4. Conclusion

In this work, graphene oxide was successfully synthesized via oxidation of pure graphite and then functionalized with dodecyl amine following with chemical reduction using hydrazine hydrate. Thermal treatment of graphene oxide was also employed to directly achieve pure graphene. The synthesized materials as well as reference samples were characterized using different methods. The obtained results were conducted to the following conclusion:

- The results of elemental analysis in conjunction with the results of FTIR measurements showed that using oxidation of pure graphite via Hummers' method led to a valuable extent of oxidation and creation of different oxygen containing functional groups on graphite surface. Moreover, the type and the extent of different oxygen containing functional groups were determined using the XPS analysis.
- Using the FTIR and XPS analyses it was demonstrated that the grafting of dodecyl amine chains were taken place by an esterification and amidation reactions of carboxyl and epoxy groups of graphene oxide sheets. The grafting of dodecyl amine chains onto graphene oxide sheets manifested itself in alteration of thermal stability, XRD patterns and Raman spectrums. It was also shown that the amine functions of dodecyl amine chains could act as a reduction agent during the grafting process.
- Structural changes of the materials during different stages of modification were also reflected in their amphiphilic characteristics and morphological features, evaluated using the contact angle experiments and SEM analysis, respectively.
- Thermally reduced and exfoliated graphene oxide exhibited near pure graphene characteristics by means of TGA and Raman analyses.

References

[1] X. Huang, Z. Yin, Sh. Wu, X. Qi, Q. He, Q. Zhang, Q. Yan, F. Boey and H. Zhang, *Small*, 2011, **7**(14), 1876–1902

[2] J. Luo, J. Kim, and J. Huang, *Acc. Chem. Res.*, 2013, **46** (10), 2225–2234

[3] H. Kim, A. A. Abdala and Ch. W. Macosko, *Macromolecules*, 2010, **43**, 6515–6530

[4] D. Lahiri, R. Dua, Ch. Zhang, I. d. S. Novoa, A. Bhat, Sh. Ramaswamy, and A. Agarwal, *ACS Appl. Mater. Interfaces*, 2012, **4**, 2234−2241

[5] D. K. James and J. M. TOUR, *Accounts of chemical research*, 2013, **46** (10), 2307–2318

[6] T. K. Das and S. Prusty, *Polymer-Plastics Tech. Eng.*, 2013, **52**, 319–331

[7] Y. Lin, J. Jin, O. Kusmartsevab, and M. Song, *J. Phys. Chem.*, 2013, **117**, 17237−17244

[8] X. Wang, W. Xing, P. Zhang; L. Song, H. Yang and Y. Hu, *Composites Science and Technology*, 2012, **72**, 737–743

[9] H. B. Zhang, W. G. Zheng, Q. Yan, Z. G. Jiang and Zh. Zh. Yu, *Carbon*, 2012, **50**(5), 5117 –5125

[10] M. Castelaín, G. Martínez, C. Marco, G., and H. J. Salavagione, *Macromolecules*, 2013, **46**, 8980−8987

[11] V. Singh, D. Joung, L. Zhai, S. Das, S. I. Khondaker and S. Seal, *Progress Mater. Sci.*, 2011, **56**, 1178–1271

[12] B. Yuan, Ch. Bao, L. Song, N. Hong, K. M. Liew and Y. Hu, *Chemical Engineering Journal*, 2014, **237**, 411–420

[13] K. I. Sasaki, M. Yamamoto, Sh. Murakami, R. Saito, M. S. Dresselhaus, K.Takai, T. Mori, T. Enoki, and K. Wakabayashi, *Phys. Rev.*, 2009, **80**, 15451-15462

[14] J. Liu, R. Wang, L. Cui, J. Tang, Zh. Liu, Q. Kong, W. Yang, and J. Gooding, *J. Phys. Chem.,* 2012, **116**, 17939−17946

[15] D. C. Marcano, D. V. Kosynkin, J. M. Berlin, A. Sinitskii, Zh. Sun, A. Slesarev, L. B. Alemany, W. Lu and J. M. Tour, *J. Am. Chem. Soc.*, **4** (8), 4806–4814

[16] D. R. Dreyer, S. Park, Ch. W. Bielawski and R. S. Ruoff, *Chem. Soc. Rev.*, 2010, **39**, 228–240

[17] S. Kochmann, T. Hirsch and O. S. Wolfbeis, *Trends in Analytical Chemistry*, 2012, **39**, 87-113

[18] H. R. Mamaqani, V. H. Asl, Kh. Khezri and M. S. Kalajahi, *RSC Adv*., 2014, **4**, 24439–24452

[19] A. Hirsch, J. M. Englert, and F. Hauke, *Acc. Chem. Res.*, 2013, **46** (1), 87–96

[20] K. Liu, Sh. Chen, Y. Luo, D. Jia, H. Gao, G. Hu and L. Liu, *Composites Sci. Tech.*, 2013, **88**, 84–91

[21] M. Quintana, E. Vazquez and M. Prato, *Acc. Chem. Res.*, 2013, **46** (1), 138–148

[22] A. Guimont, E. Beyou, P. Alcouffe, Ph. Cassagnau, A. Serghei, G. Martin and Ph. Sonntag, *Polymer*, 2014, **55**, 22-28

[23] H. R. Mamaqani, V. H. Asl, Kh. Khezri and M. S. Kalajahi, *Polymer Eng. Sci.*, 2015, **55**(8), 1720-1732

[24] F. Samadaei*,* M. S. Kalajahi, H. R. Mamaqani and M. Banaei, *RSC Adv.*, 2015, **5**, 71835–71843

[25] T. Kuila, P. Khanra, A. K. Mishra, N. H. Kim and J. H. Lee, *Polymer Testing*, 2012, **31**, 282–289

[26] P. G. Ren, H. Wang, H. D. Huang, D. X. Yan and Zh. M. Li, *J. Appl. Polymer. Sci.*, 2014, **131**(2), 39803-39811

[27] A. A. Vasileiou, M. Kontopoulou and A. Docoslis, *ACS Appl. Mater. Interfaces* 2014, **6**, 1916−1925

[28] R. J. Seresht, M. Jahanshahi, A. M. Rashidi and A. A. Ghoreyshi, *Iranica J. Energy & Environ.*, 2013, **4** (1), 53-59

[29] S. Pei and H. M. Cheng, *Carbon*, 2012, **50**(9), 3210-3228

[30] C. Botas, P. Álvarez, P. Blanco, M. Granda, C. Blanco, R. Santamaría, L. J. Romasanta, R. Verdejo, M. A. L. Manchado and R. Menéndez, *Carbon*, 2013, **65**, 156 –164

[31] J. Chen, B. Yao, Ch. Li and G. Shi, *Carbon*, 2013, **64**, 225–229

[32] H. Kim, Sh. Kobayashi, M. A. Abdurrahim, M. J. Zhang, A. Khusainova, M. A. Hillmyer, A. A. Abdala and Ch. W. MacOsko, *Polymer*, 2011, **52**, 1837-1846

[33] F. Beckert, A. M. Rostas, R. Thomann, S. Weber, E. Schleicher, Ch. Friedrich, and R. Mülhaupt, *Macromolecules,* 2013, **46**, 5488−5496

[34] L. B. Zhang, J. Q. Wang, H. G. Wang, Y. Xu, Zh. F. Wang, Zh. P. Li, Y. J. Mi and Sh. R. Yang, *Composites*, 2012, **43** (A), 1537–1545

[35] Z. Tang, H. Kang, Z. Shen, B. Guo, L. Zhang, and D. Jia, *Macromolecules,* 2012, **45**, 3444−3451

[36] S. H. Shim, K. T. Kim, J. U. Lee and W. H. Jo, *ACS Appl. Mater. Interfaces*, 2012, **4**, 4184−4191

[37] H. Hu, Ch. C. K. Allan, J. Li, Y. Kong, X. Wang, J. H. Xin and Hong Hu, *Nano Res.*, 2014, **7**(3), 418-433

[38] A. M. Shanmugharaj, J. Yoon, W. Yang and Sh. Ryu, *J. Colloid Interface Sci.*, 2013, **401**, 148–154

[39] I. Childres, Raman spectroscopy of graphene and related materials, *Book*, chapter **19**

[40] I. Calizo, D. Teweldebrhan, W. Bao, F. Miao, C. N. Lau, and A. A. Balandin, *J. Phys.*, 2008, **109**

[41] F. Tuinstra and J. L. Koenig, *J. Chem. Phys.*, 1970, **53**, 1126

[42] L. Gao, W. Ren, B. Liu, R. Saito, Zh. Sh. Wu, Sh. Li, Ch. Jiang, F. Li and H. M. Cheng, *ACS Nano*, 2013, **3** (4), 933–939

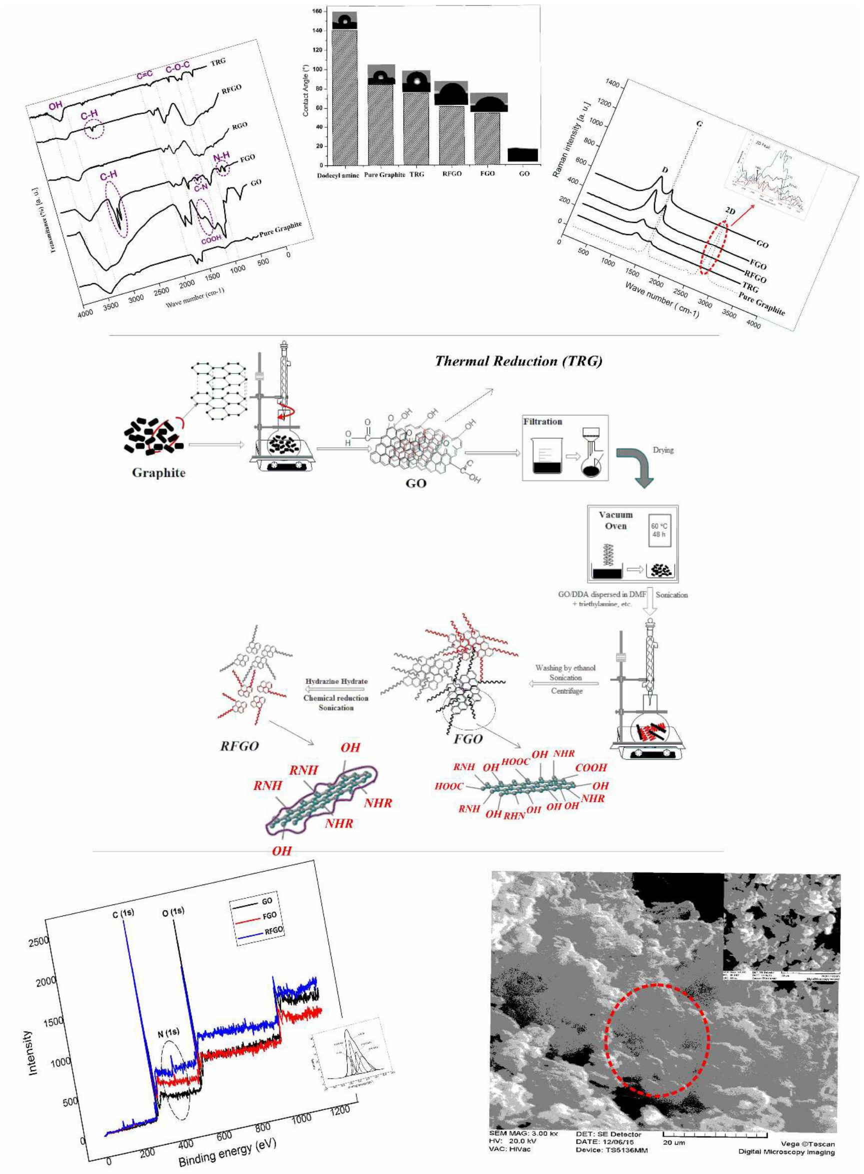
OH
C-H
C=C
C-O-C
TRG
RFGO
RGO
N-H
FGO
C-N
GO
COOH
Pure Graphite
Transmittance (%) [a. u.]
Wave number (cm-1)
Contact Angle (°)
Dodecyl amine
Pure Graphite
TRG
RFGO
FGO
GO
Raman intensity [a. u.]
Wave number (cm-1)
D
G
2D
Thermal Reduction (TRG)
Graphite
GO
Filtration
Drying
Vacuum Oven
60 °C 48 h
GO/DDA dispersed in DMF + triethylamine, etc.
Sonication
Washing by ethanol
Sonication
Centrifuge
Hydrazine Hydrate
Chemical reduction
Sonication
RFGO
FGO
OH
RNH
NHR
HOOC
COOH
RHN
Intensity
Binding energy (eV)
C (1s)
O (1s)
N (1s)
SEM MAG: 3.00 kx
HV: 20.0 kV
VAC: HiVac
DET: SE Detector
DATE: 12/06/15
Device: TS5136MM
20 um
Vega ©Tescan
Digital Microscopy Imaging